Indian Journal of Pure & Applied Physics
Vol. 61, May 2023, pp. 366-374
DOI: 10.56042/ijpap.v61i5.68768

Determination of Electron Mobility in Small Molecular 1,4-di(bis(8-hydroxyquinoline)aluminum-oxy)benzene by Transient Electroluminescence

Aparna Tripathi[a*] & Pankaj Kumar[b]

[a]Department of Applied Sciences, National Institute of Technology Delhi, New Delhi 110 040, India

[b]CSIR-National Physical Laboratory, Dr. K. S. Krishnan Marg, New Delhi 110 012, India

Received 17 November 2022; accepted 28 March 2023

Transient electroluminescence is an important tool to determine the charge carrier dynamics in light emitting organic semiconductors. We have used this method to determine the electron mobility in one of the important organic semiconductors 1,4-di(bis(8-hydroxyquinoline)aluminum-oxy)benzene (Alq(1)), used as emissive layer in organic light emitting diodes (OLEDs). For transient electroluminescence studies, we prepared OLEDs using Alq(1) as the emitter. The OLEDs were prepared on indium tin oxide (ITO) coated glass substrates using *N*, *N'*-diphenyl -*N*,*N'*- bis (3-methylphenyl)-(1,1'-biphenyl)-4,4- diamine (TPD) as hole transport layer (HTL) and lithium fluoride (LiF) as electron injecting buffer layer. The temporal evaluation of the electroluminescence (EL) was studies with respect to a voltage pulse of different amplitudes applied to the device at different temperatures. A delay was observed in the onset of EL from the device with respect to the applied voltage pulse. The EL exhibited a fast initial rise followed by tending to saturate. The EL decayed rapidly as the applied voltage became zero and the decay did not depend upon the amplitude of the applied voltage pulse. The delay time in the onset of EL with respect to the applied voltage pulse is correlated to the electron mobility in Alq(1). The electron mobility in Alq(1) calculated by transient EL method, showed strong dependency on the applied electric field and temperature at low electric fields however at quite high electric fields, the electron mobility in Alq(1) showed poor dependency on the applied electric field and temperature. This behavior of electron mobility in Alq(1) has been explained in terms of shallow charge carrier traps in Alq(1) film. The electron mobility in Alq(1) at 295 K and 2.7×10^{6} V/cm, has been determined to be 5.4×10^{-6} $cm^2V^{-1}s^{-1}$, which is much higher than that in the well-studied Alq_3.

Keywords: Organic light emitting diodes; Hole transport layer; Transient electroluminescence; Electron mobility; 8-hydroxyquinoline derivative; Soluble small molecule

1 Introduction

Since the discovery of quite high conductivity in conjugated organic materials[1], serious efforts are being continuously made globally to develop organic electronic devices and to make them commercially viable. These devices incorporate organic semiconductors as the active medium for the operation and functioning of the devices. Organic semiconductors find applications in important devices like light emitting diodes, lasers, solar cells, thin film transistors, integrated circuits (ICs), biosensors *etc*[1-6], and have the potential to replace those based on conventional inorganic semiconductor and revolutionize the electronic sector with modern and advanced applications. Organic electronic devices promise to be highly cost effective, thin, light weight and mechanically flexible. They are easy to manufacture and have found enormous applications. Extensive research and development in OLEDs has taken them to the market place and OLEDs are available as display screens in a number of electronic devices like, televisions, laptops, mobile phones, music players, digital cameras *etc*[7]. Intense research is now being done to make white OLED panels large and efficient enough for general lighting purposes. OLEDs is the only technology based on organic semiconductors that is now available in the international market but the other technologies like solar cells, lasers, biosensors, transistors or ICs are still in the laboratories and it will take some time for them to come into the international market because their performance is still not high enough to sought the commercialization. The performance of these devices directly depends upon the properties of the organic semiconductors they use. Tailoring of organic molecules towards better optical and electrical

*Corresponding author: (E-mail: apdjtripathi@gmail.com)

properties would result in better device performance. The electronic properties of organic semiconductors are normally inferior than inorganic semiconductors but to improve them it becomes very important that they are determined by extensive materials analysis.

Extensive experiments have been performed to understand the charge transport phenomenon in organic semiconductors and it is observed that the charge transport phenomena in organic semiconductors are not universal but it depends upon the materials characteristics and their operating conditions[8,9]. Charge carrier mobility is an important parameter and it plays a very crucial role in controlling the performance of organic electronic devices. The mobility of charge carriers in organic semiconductors is also a debatable parameter and its behavior varies material to material. The charge carrier mobility in organic semiconductors is very low compared to that in inorganic semiconductors, therefore the injected charge carriers form a space charge in organic semiconductors that controls the current conduction and the conduction is known as space charge limited conduction (SCLC). The organic semiconductors are usually amorphous in nature and have lots of traps, which could be Gaussianly distributed or Exponentially distributed in energy space[1]. The SCLC is affected by charge carrier traps and Kumar *et al.* have proposed models to interpret the observed current-voltage (*I-V*) characteristics in such cases[10-12]. In brief the SCLC in organic semiconductors is either interpreted (i) in terms of drift of charge carriers in the extended states, where mobility is considered to be independent of electric field or temperature, or (ii) in terms of hoping of charge carriers from one site to other site with electric field and temperature dependent mobility. In the literature, the two charge transport models have been known as the band model and the mobility model respectively[1]. In the mobility model the charge carrier mobility shows exponential dependence on the square root electric field. For the better understanding of charge transport phenomenon and mobility in organic semiconductors more and more experiments should be performed by different methods. The charge carrier mobility in organic semiconductors could be determined by a number of ways like making single carrier devices by sandwiching the semiconductor between two electrodes in such a way that the electrodes allow only one type of charge carriers to pass through the material[13,14], by time of flight (TOF) method[15] and by transient electroluminescence[16]. The field effect transistor devices can also help in determination of mobility of charge carriers but they give the surface mobility of charge carriers, which are much higher than their bulk mobility[17].

TOF method is an important technique to determine the charge carrier mobilities in organic semiconductors. In this method a thin charge sheet is generated in the organic semiconductor by optical excitation and allowed to move within the semiconductor under the effect of externally applied electric field. For the non-dispersive charge transport if the transit time of the photo-generated charge sheet within the semiconductor film from one end to other could be determined, one can easily calculate the charge carrier mobility (μ) by using the following equation,

$$\mu = \frac{L^2}{\tau_t V} \tag{1}$$

where L is the semiconductor thickness, V is the applied voltage across the semiconductor film and τ_t is the transit time of the charge sheet through the semiconductor film. But Eq. (1) does not tell the temperature or electric field dependence of the mobility. According to the mobility model, the temperature and electric field dependence of the charge carrier mobility in organic semiconductors can be given as

$$\mu(E,T) = \mu_{00} \exp\left(-\frac{\Delta}{k_B T} + \beta\left(\frac{1}{k_B T} - \frac{1}{k_B T_0} \right)\sqrt{E} \right) \tag{2}$$

where μ_{00} is a constant, k_B is the Boltzmann constant, T is the absolute temperature, Δ is the zero-field activation energy, T_0 is temperature shift factor ranging from 300-600 K, β is of Poole-Frenkel like coefficient and E is the applied electric field. The mobility model assumes disorder induced localization and the charge carriers hop from one localized state to another. The inter-molecular hopping of charge carriers can be easily increased either by increasing the externally applied electric field or by thermal excitation or by both. But this method has some limitations and proved to be a little problematic for electron transport[18,19].

Transient electroluminescence is another important method which could be used to determine the charge carrier mobilities in light emitting organic semiconductors. For that purpose, one need to make an

OLED using the material to be studied and apply a square voltage pulse across the OLED. The voltage pulse injects the electrons and holes which transport through the respective charge transport layers and light emitting layer that radiatively recombine at the emitter interface and lead to the light emission. The transient studies of the EL with respect to the applied voltage pulse help to understand the charge carrier injection, transportation and their recombination. To understand the transient EL in the bilayer OLEDs, Nikitenko *et al.* proposed a theoretical model, which is known as Marburg Model[20]. It is observed that after a voltage pulse is applied to the OLED, it takes a while for light emission from the device. This delay in light emission is basically correlated to the time required for the charge carriers to transport through the emissive layer and recombine at the emitter interface[21]. Fig. 1(a) shows schematically the structure of a typical OLED and Fig, 1(b) shows its working mechanism through schematic energy level diagram. In brief, the OLEDs are prepared on transparent conducting electrodes like indium tin oxide (ITO) coated substrates. ITO is coated with a hole transport layer (HTL), which is followed by the deposition of light emitting layer. On the top of the light emitting layer a thin layer of electron injection layer (EIL) is deposited and finally a top metal electrode is deposited to complete the device. When a voltage is applied across the device (+ve bias to anode and –ve bias to cathode), the electrons and holes are injected into the device from anode and cathode respectively. The holes are injected from anode into highest occupied molecular orbital (HOMO) of HTL and transport through it to reach the HTL/emitter interface whereas electrons are injected from cathode into lowest occupied molecular orbital (LUMO) of emissive layer through EIL and transport through the emissive layer to reach at the HTL/emitter interface and recombine there with the holes to emit light. Depending upon the electron/hole mobility in the emitter the recombination could take place at the HTL/emitter interface or emitter/EIL interface.

After a voltage is applied across the OLED, the delay in EL can be considered as the sum of two-time intervals; (i) the delay in charge injection (t_{inj}) and (ii) the delay in charge transportation (t_{trans}) before the recombination at the interface. The delay time in EL (t_d) can be written as

$$t_d = t_{inj} + t_{trans} \tag{3}$$

The OLEDs can be considered a kind of capacitive devices as they have two electrodes and the organic materials sandwiched between them works as the dielectric medium. In such a condition the t_{inj} can be considered as the charging time of the capacitor and can be given by

$$t_{inj} = RC \ln\left(\frac{V_{\max}}{V_{\max} - V_{th}}\right) \tag{4}$$

where, RC is the capacitor time constant, $V_{\max}$ is the voltage pulse amplitude and V_{th} is the threshold voltage for charge injection[22]. Once the delay time in EL is measured the charge carrier mobility can be calculated from the following relationship,

$$t_d = \frac{d_e}{(\mu_e + \mu_h)E} \tag{5}$$

where d_e is the distance travelled by the electrons and holes before recombination, μ_e and μ_h are the electron and hole mobilities respectively and E is the internal electric field in the device. As it is difficult to measure both the electron and hole mobilities simultaneously, the transient EL method is used for the materials where mobility of one type of charge carriers is more than the other. In that case, one of the mobilities in Eq. (5) can be ignored and the calculation becomes simpler. For example, if the electron mobility is more than hole mobility ($\mu_e >> \mu_h$), and the internal electric field is considered to be $(V\text{-}V_{bi})/d$ then Eq. (5) can be written as,

$$t_d = \frac{d_e d}{\mu_e (V - V_{bi})} \tag{6}$$

where V is the amplitude of the applied voltage pulse, V_{bi} is the internal built-in potential and d is the thickness of the whole organic layers. Usually, small molecular organic semiconductors exhibit higher electron mobilities than the hole mobility whereas polymeric organic semiconductors exhibit higher hole mobility than the electron mobility.

In this paper we present the transient EL studies carried out on one of the important small molecular organic semiconductors 1,4-di(bis(8-hydroxyquinoline) aluminum-oxy) benzene Alq (1). We synthesized Alq(1) along with some other derivatives of 8-hydroxyquinoline and compared the performance with another well studied small molecular green light emitting material tri(8-hydroxyquoniline) aluminium

(Alq_3)[23]. Alq(1) showed not only better EL efficiency compared to Alq_3 but it was also soluble in common organic solvent and led to fabrication of OLEDs via solution processing, which was not possible with Alq_3. Alq_3 is well studied as electron transport layer and green light emitter in OLEDs with broad emission peak at 530 nm[24]. We have published a detailed characterization of Alq(1) and fabricated OLEDs using it as a replacement of Alq_3[23]. Alq(1) exhibited green light emission with peak position at 520 nm and outperformed Alq_3 in terms of optical, electrical and thermal properties. Alq(1) was proposed as a better electron transport materials (ETM) and green emitter than Alq_3. Though we did not measure the electron mobility in Alq(1) before, but better EL efficiency in Alq(1) devices was attributed to its better electron mobility than Alq_3. We now present here the studies performed to measure the electron mobility in Alq(1) via transient EL method.

2 Experimental Details

To determine the electron mobility in Alq(1), the OLEDs were prepared on ITO coated glass substrates (resistivity ~ 18 Ω/Sq) in the bilayer structure ITO/TPD/Alq(1)/LiF/Al. Here TPD works as HTL, LiF works as EIL and ITO and Al work as anode and cathode respectively. The schematic structure of fabricated OLEDs can be represented by the one shown in Fig. 1 (a), where HTL would be TPD and the emissive layer would be Alq(1). The molecular structures of TPD and Alq(1) are shown in Fig. 1 (c). Prior to any deposition the ITO coated glass substrates were cleaned via standard cleaning procedure, which included sequential washing with soap solution, distilled water, acetone and iso-proponol. The substrates were dried in a vacuum oven at 100 °C for 15 min. The cleaned ITO coated glass substrates were exposed to air plasma treatment for 15 min. in a vacuum chamber. 20 nm thin film of TPD was deposited on ITO substrates by thermal evaporation in a vacuum chamber that was followed by 30 nm deposition of Alq(1) on TPD and 0.5 nm deposition of LiF on Alq(1) and 150 nm deposition of top Al electrode on LiF. All the thermal evaporations were carried out at a base pressure of 5×10^{-6} Torr. Al electrodes were deposited through shadow masks, with the defined active area of 4 mm^2. The devices were transferred to a liquid nitrogen cryostat where they were mounted on a Cu block which was cooled from 295 K to 150 K using liquid nitrogen. To avoid any condensation of moisture on the samples, the whole assembly was placed in the vacuum chamber at 3×10^{-3} Torr. Considering the OLED to be a capacitor, the series resistance and capacitance of the Alq(1) OLED were determined to be 76 Ω and 1.1 nF and the overall time constant *RC* was determined to be less than 0.1 μs using an impedance analyzer.

Figure 2 shows the schematic of the experimental setup used to study the transient EL in Alq(1) OLED. The experimental setup consisted of a function generator, which was used to generate square voltage pulses to excite the OLEDs, a photo-multiplier tube

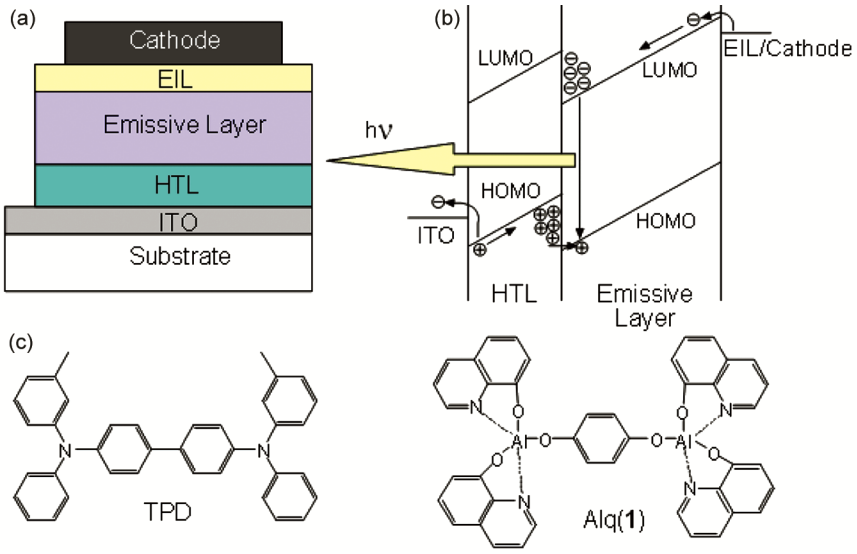

Fig. 1 — (a) Schematic representation of the OLEDs prepared to study the transient electroluminescence. In the present studies the HTL was TPD, the emissive layer was Alq(1), EIL was LiF and the cathode was made of Al. (b) Schematic representation of the working mechanism of the OLEDs studied here. (c) Molecular structures of TPD and Alq(1) materials.

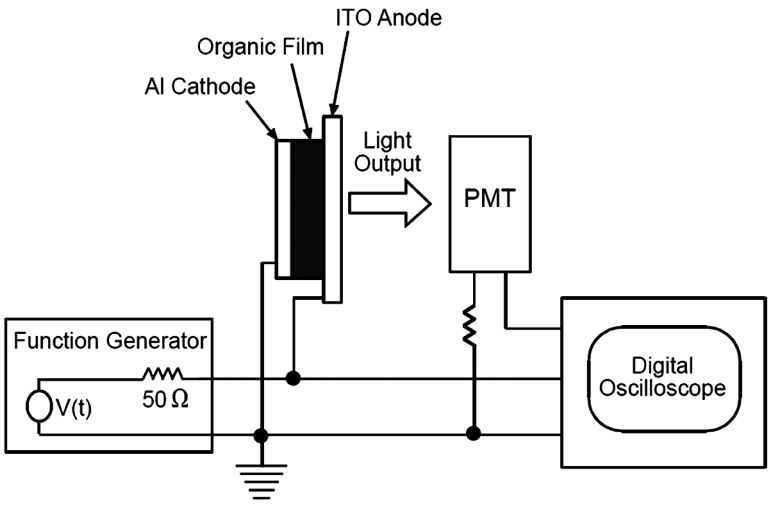

Fig. 2 — Schematic representation of the experimental setup used to study the transient electroluminescence.

(PMT), which was used to detect the emitted light from the OLEDs and a digital oscilloscope to read the wave forms of the voltage pulse and the emitted light from the OLEDs. For these studies we used HAMEG HM8131-2 function generator to generate square electrical pulses of different amplitudes and HAMEG Analog-Digital Scope HM1507-3 oscilloscope to read the waveforms, rise and decay time in EL. The OLEDs were applied different voltage pulses with frequency of 5 KHz and, duty cycle of 50%. The time resolved EL response was measured using the PMT detector. The output of the PMT detector was coupled with one of the input channels of the oscilloscope, whereas the output of the function generator was fed to the OLED and the other input channel of the oscilloscope. The input voltage pulse to the OLED and the output EL response of the OLED were recorded simultaneously on the oscilloscope. The overlapping of the input voltage pulse and output EL response led to determine the delay in the onset of the EL.

3 Results and discussion

Figure 3 shows the profiles of the applied input voltage pulse to one of the OLEDs and its transient EL response on the time scale measured with the oscilloscope. A delay (t_d) in the onset of EL after application of voltage pulse can be clearly seen form the figure. Basically, this delay time is associated with the time required in transportation of charge carriers, excitons formation and recombination. In general, this delay time is considered to be the time required for the leading front of the charge carriers to transport and recombine with opposite charge carriers at the emitter interface[25]. The forward bias (+ve bias at anode) results

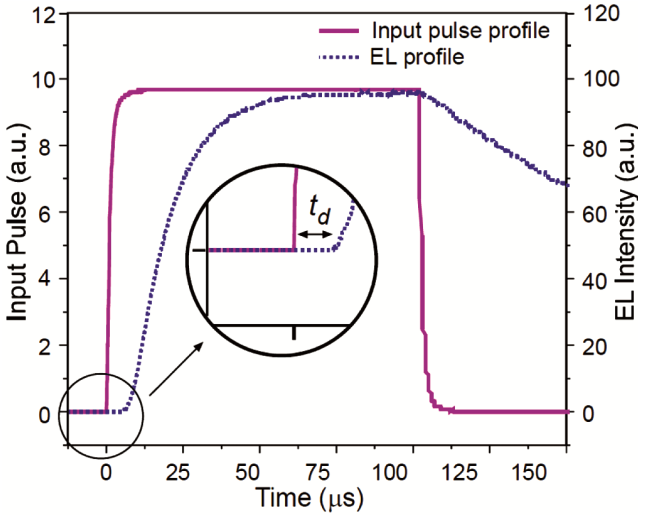

Fig. 3 — Transient profiles of the applied voltage pulse and the corresponding EL on the time scale. Inset shows the magnified image of the circled region and the delay time t_d between applied voltage pulse and the onset of EL can be seen clearly.

in injection of holes from ITO into HOMO of TPD and injection of electrons from Al into LUMO of Alq(1) through LiF. Since TPD exhibits very high hole mobility of ~10^{-3} $cm^2V^{-1}s^{-1}$ [25], the holes injected from ITO quickly reach the TPD/Alq(1) interface. As Alq(1) is a 8-hydroxyquinoline derivative, it is expected to have higher electron mobility than hole mobility. The lower hole mobility in Alq(1) and the interface barrier at the TPD/Alq(1) leads to accumulation of holes at the TPD/Alq(1) interface. This accumulation of holes at the TPD/Alq(1) interface results in building up of space charge and increment in the electric field across Alq(1) layer. This enhanced electric field across Alq(1) enhances the injection of electrons from LiF/Al

electrode into LUMO of Alq(1) and transport through Alq(1) to reach at the TPD/Alq(1) interface and accumulate there due to high barrier for electron injection from Alq(1) to TPD. Here TPD works as an electron blocking layer. The accumulation of electrons and holes across the TPD/Alq(1) interface creates very high electric field across the interface and this electric field assists the holes to tunnel into Alq(1) and recombine with the electrons to emit light photons. The total delay in EL after voltage application is mainly because of electron transportation through Alq(1). Due to high hole mobility in TPD, it can be considered to be working as a part of the anode and the voltage drop across TPD layer would be negligibly small[26] also the transit time of holes to reach the TPD/Alq(1) interface would be negligible. It can be considered that the total applied voltage is dropped across the Alq(1) layer and the delay time in EL is because of transit time of electrons through Alq(1) and meet the holes at the TPD/Alq(1) interface. The total distance travelled by electrons would be the thickness of Alq(1). In this condition the effective thickness of the device (d) can be considered to be as thickness of Alq(1) (d_e) and Eq. (6) would become

$$t_d = \frac{d_e^{\,2}}{\mu_e (V - V_{bi})} \qquad (7)$$

The delay time in the onset of EL in the present devices is observed to be on the scale of μs and the injection delay time calculated from Eq (4) is found to be less than 0.1 μs, which was negligible compared to the total delay time in the onset of EL, therefore the total delay time in the devices can be attributed to the charge carrier transport only. The EL starts decreasing as soon as the applied voltage goes OFF. There was no delay observed in the EL decay. This was because EL decay happens due to removal of charges, which does not depend upon the applied voltage.

Figure 4 shows the transient EL response of the Alq(1) OLED measured with voltage pulses of different amplitudes at 295 K. The voltage pulse shown in Fig. 4 is the normalized pulse and is same for all the applied voltages, whereas the EL profiles at different voltages are the actual profiles. The onset of EL was observed to depend upon the applied voltage. As the applied voltage increased, the delay in the onset of EL decreased. The reduction in delay time with increment in applied voltage indicates that the applied voltage helps the electrons to move faster through Alq(1) and recombine with holes at the TPD/Alq(1) interface. Faster movement can be attributed to the enhanced mobility of electrons in Alq(1). Considering the work function of ITO to be 4.8 eV and that of LiF/Al to be 3.6 eV, the built-in voltage (V_{bi}) in the present device comes out to be 1.2 eV. For better understanding, we measured the transient EL of the OLED at different voltages and different temperatures. Considering the V_{bi} of the device to be 1.2 eV, the measure values of delay time (t_d) have been plotted in Fig. 5 as a function of effective electric field $\{(V\text{-}V_{bi})/d_e\}$ at different temperatures. Symbols represent the measured delay time at different temperatures and

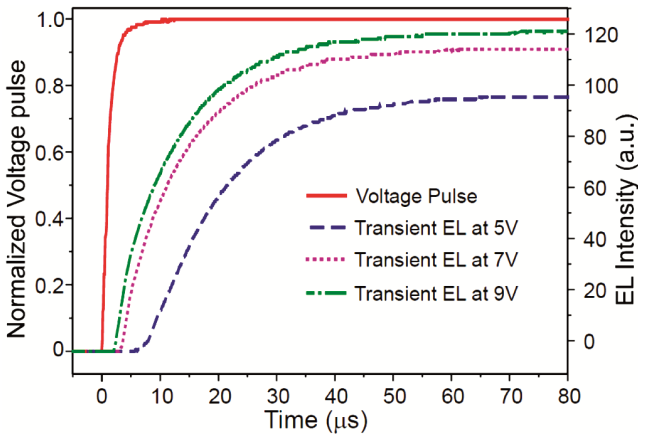

Fig. 4 — The transient profiles of the applied voltage pulse and the EL at different voltages measure at 295 K. The voltage profile showed here is the normalized one and the same for all voltages.

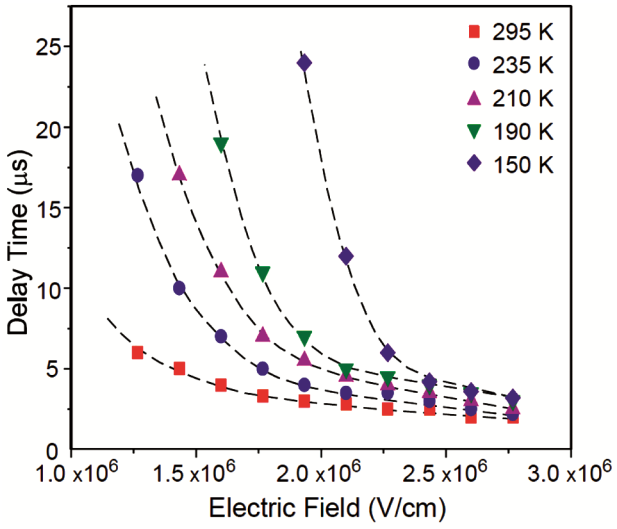

Fig. 5 — The measured delay time in the onset of EL (t_d) plotted as a function of effective electric field in the device at different temperatures. Symbols represent the experimental data whereas dashed curves have been plotted just to guide the eyes about the trend of variation of the delay time with electric field.

electric fields, whereas the dashed curves have just been plotted to guide the eyes about the trend of delay time with electric field and temperature variation. These experiments were performed at different temperatures in the range 150-295 K and different applied voltages in the range 5-10 V. For a given temperature the delay time increases as the effective electric field decreases. As the temperature decreased the delay time in the onset of EL increased at a given electric field. The increment in the delay time with reduction in the applied electric field takes place more rapidly at lower temperatures than that at higher temperatures. The delay time showed non-linear dependence on electric field. According to Eq. (7), the non-linear dependence of the delay time on the electric field and temperature suggests that the mobility is a function of electric field and temperature. It appeared that the delay time at all the temperatures tended to merge with each other and become independent of electric field at quite high electric fields. At quite high electric fields the delay time tends to become independent of both the temperature and electric field. The independence of delay time with the temperature and applied electric field can be understood from the fact that at quite high electric fields the charge carriers attain quite high mobility and transport through the organic layer very fast, leading to negligible delay in the onset of EL. As the organic semiconductors are full of traps, at quite high electric fields, even at the low temperatures, the charge carriers trapped in the trap sites get sufficient energy to come out of the traps and transport through the organic layer as if there were no traps. This can be better understood from the temperature and electric field dependence of the charge carrier mobility. To determine the effect of electric field and temperature on the electron mobility, we calculated it at different temperatures and electric fields using Eq. (7). The calculated values of electron mobility were compared with the electric field and temperature dependence of mobility as per Eq. (2).

Figure 6 shows the plots of calculated electron mobility in Alq(1) as a function of square root of effective electric field at different temperatures. Symbols represent the experimental data whereas solid lines are the plots of Eq. (2) at the corresponding temperatures. The electron mobility in Alq(1) has also been observed to be function of effective electric field and the temperature. The experimental data showed a reasonable good fitting with the mobility values calculated from Eq. (2). The values of different fitting parameters were found to be Δ = 0.295 eV, μ_{00} = 9x10^{-2} cm^{2}V^{-1}s^{-1}, β = 1.75x10^{-4} (V/cm)$^{1/2}$eV^{-1}, and T_0 = 370 K. At 295K, the electron mobility in Alq(1) was found to be in the range 3.9×10^{-6} – 5.4×10^{-6} cm^{2}V^{-1}s^{-1} for the electric field 1.2×10^6 – 2.7×10^6 V/cm. The electron mobility in pure Alq_3 material is found to be around 1×10^{-6} cm^{2}V^{-1}s^{-1} [27]. Present studies clearly suggest that Alq(1) has better electron mobility compared to well studied Alq_3. These studies are in quite good agreement with the previous studies performed on Alq(1) and Alq_3 OLED devices, as Alq(1) OLEDs exhibited better efficiency compared to Alq_3 OLEDs[23]. The electron mobility in Alq(1) at low electric fields showed strong dependence upon the electric fields and temperature. The electric field and temperature dependence of the electron mobility in Alq(1) at lower electric fields can be understood from the fact that most organic semiconductors are amorphous in nature and are full to defects, which work as charge carrier traps in the semiconductor films[1,2]. The charge carrier traps could be distributed Gaussianly or exponentially in energy space and they could be shallow or deep in energy. The charge carrier traps capture the charge carriers and hamper their mobility in the semiconductor. Due to charge carrier traps, the semiconductors allow relatively lower current to pass through them. For the trapped charge carriers to contribute to the current they need to come out of the traps and for that

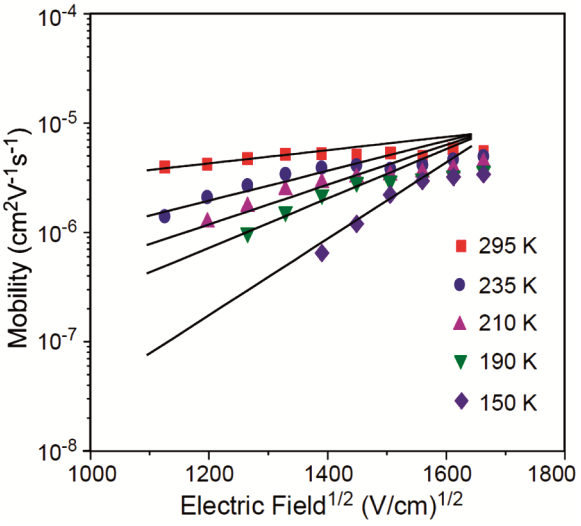

Fig. 6 — Calculated electron mobility plotted against the square root of effective electric field at different temperatures. Symbols represent the experimental data whereas solid lines are the plots of Eq. (2) at the corresponding temperatures.

purpose the charge carriers require extra energy to take them out of the traps. This extra energy could be provided either by thermal energy or by electric field or by both. At low electric fields and low temperatures, the charge carriers do not get sufficient energy to come out of the traps and they do not contribute to the current and always remain in the traps. The trapped charge carriers form space charge that provides a screening force for the next coming charge carriers and reduce their mobility. Due to charge carrier traps in the organic semiconductors the charge carrier mobilities are low at low temperatures and low electric fields. As the electric field and temperature increases, some of the trapped charge carriers might get sufficient energy to come out of the traps and contribute to current flow. In this case the reduced amount of space charge would not only increase the amount of current flowing through the sample but it will also increase the mobility of charge carriers flowing through the semiconductor. The same concept is applied here and the increment in electric field and temperature results in the increment in both the current flowing through the device and the electron mobility in Alq(1). Due to increment in the electron current with increment in the electric field, the electron hole recombination at the TPD/Alq(1) interface increases that leads to early onset of EL and increment in the EL intensity (Fig. 4).

For quite high electric fields more than 2.3×10^6 V/cm, the mobility showed poor dependence on the electric field and the temperature. For quite high electric fields the mobility values tend to merge into each other and become independent of electric field and temperature. This poor temperature and electric dependency of the electron mobility in Alq(1) at quite high electric fields can be understood from the fact that high electric fields all the trapped charge carriers get released from the traps and they move in the semiconductor through extended states very fast with negligible delay time. As there are no charge carriers trapped in the traps at high electric fields, the charge carriers move in the semiconductor as if there were no traps. At quite high electric field the electrons attain quite high mobility and sweep through the semiconductor film very fast and the mobility shows poor dependence on variation of temperature and electric field.

4 Conclusions

We have studied the electron mobility in a small molecular organic semiconductor Alq(1), by transient electroluminescence method, where a light emitting device (OLED) was prepared and Alq(1) was used as the emissive material. A voltage pulse was applied to the device and the onset of EL was studied as a function of applied electric field. A delay in onset of EL was observed which was correlated to the electron transport time in Alq(1). The transient EL studies were performed at different temperatures under a wide range of applied electric field. The delay in onset of EL at different temperatures and applied electric fields helped us to calculate the electron mobility in Alq(1). At lower electric fields the calculated electron mobility in Alq(1) showed strong dependence on the applied electric field and temperature. For a given temperature, as the applied electric field decreases the mobility decreases and for a given electric field as the temperature decreases the mobility decreases. At quit high electric field the electron mobility in Alq(1) showed poor dependence on both the temperature and applied electric field. The strong or poor dependence of the electron mobility on temperature and applied electric field in Alq(1) has been explained through trapping and de-trapping phenomena of the electrons in the semiconductor film. At 295 K, the electron mobility in Alq(1) has been found to be 5.4×10^{-6} $cm^2V^{-1}s^{-1}$ at 2.7×10^6 V/cm. The electron mobility in Alq(1) has been found to be better than that in well studied Alq_3 material. These results are in quite good agreement with other studies performed on Alq(1) and Alq_3 OLEDs. These studies suggest that Alq(1) can not only be used as emissive material in OLEDs but also as an electron transport material in OLEDs and organic solar cells in place of Alq_3 to give more efficient organic electronic devices.

Acknowledgement

Authors would like to thank Dr. M. N. Kamalasanan, Ex. Chief Scientist of CSIR-National Physical Laboratory for his support and encouragement to carry out this work. One of the authors A.T. would also like to thank Director NIT, Delhi for his encouragement and providing the laboratory infrastructure support for execution of this work.

References

1 Kumar P, Organic solar cells: Device physics, Processing, *Degradation and Prevention*, CRC press, Taylor & Francis group, USA, (2016).

2 Liao X J, Zhu J J, Yuan L, Yan Z P, Tu Z L, Mao M X, Lu J J, Zhang W W & Zheng Y X, *Mater Chem Front*, 5 (2021) 6951.

3 Zou S J, Shen Y, Xie F M, Chen J D, Li Y Q & Tang J X, *Mater Chem Front*, 4 (2020) 788.

4 Kumar P & Chand S, *Prog Photovolt: Res Appl*, 20 (2012) 377.
5 Nagamine K & Tokito S, *Sens Actuators B: Chem*, 349 (2021) 130778.
6 Yoo H, Park H, Yoo S, On S, Seong H, Im S G & Kim J J, *Nature Commun*, 10 (2019) 2424.
7 https://www.oled-info.com/lg-oled.
8 Kumar P, Misra A, Kamalasanan M N, Jain S C, Srivastava R & Kumar V, *Jpn J Appl Phys*, 45 (2006) 7621.
9 Kapoor A K, Jain S C, Poortmans J, Kumar V & Mertens R, *J Appl Phys*, 92 (2002) 3835.
10 Jain A, Kumar P, Jain S C, Kumar V, Kaur R & Mehra R M, *J Appl Phys*, 102 (2007) 094505.
11 Kumar P, Jain S C, Kumar V, Chand S & Tandon R P, *J Phys D: Appl Phys*, 41 (2008) 155108.
12 Kumar P, Jain S C, Kumar V, Chand S & Tandon R P, *Eur Phys J*, 28 (2009) 361.
13 Kumar P, Chand S, Dwivedi S & Kamalasanan M N, *Appl Phys Lett*, 90 (2007) 023501.
14 Alam S, Fischer P, Kästner C, Singh C R, Schubert U S & Hoppe H , *J Mater Res*, 33 (2018) 1860.
15 Funahashi M, *Organic semiconductors for optoelectronics*, Ed by Naito H, Wiley (2021).
16 Qiao X, Xiao S, Yuan P, Yang D & Ma D, *Front Optoelectron*, 15 (2022) 11.
17 Xu Y, Benwadih M, Gwoziecki R, Coppard R, Minari T, Liu C, Tsukagoshi K, Chroboczek J, Balestra F & Ghibaudo G, *J Appl Phys*, 110 (2011) 104513.
18 Martens H C F, Huiberts J N & Blom P W M, *Appl Phys Lett*, 77 (2000) 1852.
19 Redecker M, Bradley D D C, Inbasekaran M & Woo E P, *Appl Phys Lett*, 73 (1998) 1565.
20 Nikitenko V R, Arkhipov V I, Tak Y H, Pommerehne J, Bassler H & Horhold H H, *J Appl Phys*, 81 (1997) 7514.
21 Wang J, Sun R G, Yu G & Heeger A J, *J Appl Phys*, 91 (2002) 2417.
22 Marai F, Romdhane S, Romdhane A, Bourguigua R, Loussaief N, Fave J L, Majdoub M & Bouchriha H, *Synth Mater*, 114 (2000) 255.
23 Kumar P, Misra A, Bhardwaj R, Kamalasanan M N, Jain S C, Chand S & Tandon R P, *Displays J*, 29 (2008) 351.
24 Chan J, Rakic A D, Kwong C Y, Liu Z T, Djurišic A B, Majewski M L, Chan W K & Chui P C, *Smart Mater Struct*, 15 (2005) S92.
25 Tse S C, Tsang S W & So S K, *J Appl Phys*, 100 (2006) 063708.
26 Hiramoto M, Koyama K, Nakayama K & Yokoyama M, *Appl Phys Lett*, 76 (2000) 1336.
27 Kumar A, Srivastava R, Tyagi P, Mehta D S & Kamalasanan M N, *J Appl Phys*, 109 (2011) 114511.